

Proceeding Paper

# Optimization of Fe, Al, and Na Recovery from H<sub>2</sub>-Reduced Bauxite Residue (“Red Mud”) Using Response Surface Methodology (RSM) †

Ganesh Pilla \*, Tobias Hertel and Yiannis Pontikes

Sustainable Resources for Engineered Materials (SREMat), Department of Materials Engineering, KU Leuven, B-3000 Leuven, Belgium; tobias.hertel@kuleuven.be (T.H.); yiannis.pontikes@kuleuven.be (Y.P.)

\* Correspondence: ganesh.pilla@kuleuven.be

† Presented at the 2nd International Conference on Raw Materials and Circular Economy “RawMat2023”, Athens, Greece, 28 August–2 September 2023.

**Abstract:** Bauxite residue (BR), a solid waste generated during the Bayer process for alumina production, is a polymetallic source. This study aims to investigate the recovery of Fe, Al, and Na from H<sub>2</sub>-reduced BR pellets (under 5 vol% H<sub>2</sub> + 95 vol% N<sub>2</sub> with 45 L/h flowrate) after water leaching and magnetic separation, and to further optimize the recovery process through response surface methodology (RSM). RSM with a full factorial design was employed to evaluate the effect of process variables such as temperature (400–700 °C), time (30–120 min), and NaOH addition (10–25 wt%) for the recovery of these metals from reduced pellets. From the analysis of variance (ANOVA), the significant factors on response were identified. The Fe, Al, and Na recovery was primarily influenced by the temperature and NaOH, then the reduction time. The optimum parameters for the concurrent recovery of Fe, Al, and Na recovery were predicted to be 600 °C for 2 h with 20 wt% NaOH addition, resulting in an Fe, Al, and Na recovery of 75.8%, 84%, and 90%, respectively. The actual experimental Fe, Al, and Na recovery rates are 73.4%, 80.1%, and 87.9%, respectively. The predicted recovery rates at optimal process parameters are sufficiently accurate and within the allowable variance (<5%).

**Keywords:** bauxite residue (red mud); hydrogen; sustainability; metal extraction; response surface methodology (RSM); optimization



**Citation:** Pilla, G.; Hertel, T.; Pontikes, Y. Optimization of Fe, Al, and Na Recovery from H<sub>2</sub>-Reduced Bauxite Residue (“Red Mud”) Using Response Surface Methodology (RSM). *Mater. Proc.* **2023**, *15*, 85. <https://doi.org/10.3390/materproc2023015085>

Academic Editors: Antonios Peppas, Christos Roumpos, Charalampos Vasilatos and Anthimos Xenidis

Published: 22 March 2024



**Copyright:** © 2024 by the authors. Licensee MDPI, Basel, Switzerland. This article is an open access article distributed under the terms and conditions of the Creative Commons Attribution (CC BY) license (<https://creativecommons.org/licenses/by/4.0/>).

## 1. Introduction

In the Bayer process, about 1.5–2.5 tons of bauxite residue (BR) is generated as waste per ton of alumina, depending on the type of bauxite ore and process efficiency [1,2]. The global inventory of BR is estimated to be around 5.5 billion tons by 2022 [3,4], most of it being disposed in landfills [1]. BR’s high alkalinity and fine particle size poses a potential risk to land, ecosystems, and groundwater.

Despite the various applications of BR such as source of metals, building materials, and pigments, the utilization of BR in these areas remains limited to a small fraction (<3%) of its total yearly production [1,2]. BR typically comprises hematite (Fe<sub>2</sub>O<sub>3</sub>), diasporite (Al(OH)), boehmite (γ-AlO(OH)), gibbsite (Al(OH)<sub>3</sub>), calcite (CaCO<sub>3</sub>), rutile (TiO<sub>2</sub>), anatase (TiO<sub>2</sub>), perovskite (CaTiO<sub>3</sub>), and quartz (SiO<sub>2</sub>), as well as various aluminum–silicate and aluminum–sodium–silicate phases such as kaolinite and cancrinite [2,5]. BR is a potential polymetallic source for the recovery of different metals including rare earth elements, REEs. Therefore, extensive efforts have been undertaken to explore economic and environmentally sustainable approaches for maximizing the utilization of BR, particularly through the recovery of metals at lower temperatures [4–9]. In most studies, the single-factor method is commonly used for process optimization, while ignoring the mutual interactions among the variables. This approach leads to a deficient description of the various parameters that influence the experimental results. Numerous statistical experimental design methods have

been developed in recent times to optimize processes [10]. One of these methods, response surface methodology (RSM), has emerged as an efficient technique applied successfully across various industries, including the metal, chemical, and biological sectors [10,11]. However, there have been no reports of a specific application of RSM for the optimization of the concurrent extraction of Fe, Al, and Na from BR, based on  $H_2$  reduction at low temperatures ( $<700\text{ }^\circ\text{C}$ ) and combined water leaching–wet magnetic separation.

Therefore, the primary aim of this study is to analyze and understand the individual and interconnected relationships among process variables. By employing response surface methodology (RSM), this research seeks to establish a model that optimizes the simultaneous recovery of Fe, Al, and Na from  $H_2$ -reduced BR. Specifically, the investigation focuses on three influential input parameters: reduction temperature ( $400\text{--}700\text{ }^\circ\text{C}$ ), reduction time ( $30\text{--}120\text{ min}$ ), and NaOH addition ( $10\text{--}25\text{ wt}\%$ ). The dependent variables under consideration are the recovery rates of Fe, Al, and Na. The study delves into the modeling and optimization of these operational variables to determine their impact on the recovery of Fe, Al, and Na. The optimal process parameters are derived using the Design Expert JMP Pro V.17 software. Ultimately, this investigation contributes valuable insights to the field of optimizing the recovery of Fe, Al, and Na through a combined approach involving  $H_2$  reduction and water leaching–wet magnetic separation.

## 2. Materials and Methods

The research is based on a process flowsheet, outlined in Figure 1, that encompassed various stages. These stages included pelletization of BR with NaOH,  $H_2$  reduction of dried pellets at relatively low temperature ( $<700\text{ }^\circ\text{C}$ ), wet milling, and combined water leaching with wet magnetic separation of the slurry.

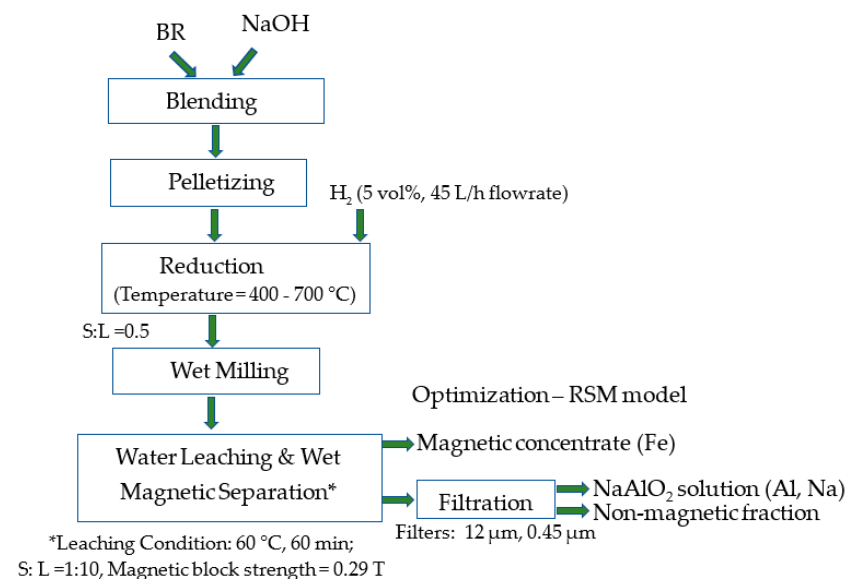


**Figure 1.** Process flowsheet followed in this research work.

The as-received BR from the Mytilineos Aluminum Greece plant was dried at  $110\text{ }^\circ\text{C}$  for 12 h in a drying oven (Memmert, Schwabach, Germany), followed by sieving ( $<500\text{ }\mu\text{m}$ ). The characterization is reported elsewhere [3,8,9,12]. For the pelletization, the BR (100 g) was mixed with NaOH solution (addition of  $10\text{--}25\text{ wt}\%$  based on dry weight, Sigma Aldrich–99.9% purity, Zedelgem, Belgium), followed by mixing/pelletization using an Eirich mixer (Type: EL1). The resulting pellets were in the size range of  $10\text{--}20\text{ mm}$ . After drying the pellets, a rectangular alumina crucible of  $100\text{ mm} \times 30\text{ mm}$  containing about 100 g of pellets was placed in a lab-scale box furnace under  $N_2$  atmosphere.

At the target temperature ( $400\text{--}700\text{ }^\circ\text{C}$ , respectively),  $H_2$  gas ( $5\text{ vol}\% H_2 + 95\text{ vol}\% N_2$ ) was purged during the specific reduction time ( $30\text{--}120\text{ min}$ ) with a flowrate of  $45\text{ L/h}$ . Then, the pellets were cooled to room temperature, maintaining a  $N_2$  atmosphere (flowrate

10 L/h) in order to avoid oxidation of reduced pellets. After reduction, the pellets were ground wet (Retsch RS200 model, Belgium) with a solid-to-liquid (S/L) ratio of 0.5. The wet-milled slurry products were subjected to water leaching/wet magnetic separation to separate water-soluble sodium aluminate solution (Al, Na recovery), magnetic (Fe recovery), and non-magnetic products (Ca, Si, Ti). The solution was kept homogeneous via constant stirring with a mechanical stirrer in a glass beaker. A solid magnet block (magnetic strength = 0.29 T) was placed inside the water-leaching set up in order to separate the magnetic product from the non-magnetic fraction. The water leaching was carried out at a temperature of 60 °C, and an S:L of 1:10 was used to avoid Si gel formation and enhance the efficiency of Fe, Al, and Na recovery. After 60 min of water leaching, the magnetic fraction was removed from the magnetic block while the remaining solid was separated from the leach liquor using a two-stage filtration step (filter papers of 12 µm and 0.45 µm). The products were characterized through WDXRF (4 kW Bruker S9 Tiger, Belgium) and ICP-OES (S8 Varian 720 ES axial, Diegem, Belgium), along with XRD (Bruker D2 Focus with Cu-K radiation from 10–50° 2θ with 0.08 step size, database: ICDD-PDF), particle size (Beckman Coulter LS 12320, California, U.S.A, suspend and dispersed with ethanol), and SEM-EDS techniques (XL 30 FEG). The formulae utilized in previous studies [8,9] to determine the recovery of Fe, Al, and Na during experiments were adopted for the calculation.

The Design Expert JMP Pro software (version 17) was employed to generate the design matrix, which is displayed in Table 1. The process variables considered in the study are reduction temperature (400–700 °C,  $x_1$ ), reduction time (30–120 min,  $x_2$ ), and NaOH addition (10–25 wt%,  $x_3$ ). In order to assess the optimum parameters and influence of different process parameters along with their interaction, the design of experiments (DoE) with statistical models was implemented. The number of experimental runs suggested through DoE was carried out in the lab and corresponding to each experimental run, the recovery rates of Fe, Al, and Na were calculated. The matrix consists of 13 experimental runs, covering all possible combinations of the independent variables. A regression model using a second-order polynomial was utilized to represent the dependent variables as a function of the independent variables.

**Table 1.** DoE matrix for reduction experiments of 5 vol% H<sub>2</sub> + 95 vol% N<sub>2</sub> with 45 L/h flowrate and recovery results of Fe, Al, and Na at different runs.

Experiment Run	Variables			Response (Experimental Data of Recovery,%)		
	Reduction Temperature (°C)– $x_1$	Reduction Time (min)– $x_2$	NaOH Concentration (wt%)– $x_3$	Fe	Al	Na
1	500	120	10	78	62	79
2	500	120	15	79	71	83
3	500	120	20	83	75	87
4	500	120	25	69	77	88
5	500	30	20	62	71	81
6	500	60	20	69	72	83
7	400	120	20	53	52	73
8	600	120	20	73	80	87
9	700	120	20	56	84	88
10	700	120	10	59	81	85
11	700	30	10	64	77	84
12	700	30	25	36	79	80
13	400	30	10	42	43	70

### 3. Results and Discussion

#### 3.1. Evaluating Model Fit

Table 2 summarizes the outcomes of the simulation. The correlation coefficient  $R^2$  can be used to determine the model's accuracy. The  $R^2$  values (Table 2) for the quadratic polynomial models for the Fe, Al, and Na recovery are 0.98, 0.98, and 0.97, respectively. These values represent the 98%, 98%, and 97% of the Fe, Al, and Na recovery results from the independent variables, respectively. Simultaneously, the adjusted  $R^2$  of the quadratic polynomial model for the Fe, Al, and Na are 0.90, 0.94, and 0.88. The adjusted  $R^2$  values indicate the goodness of a fit which will influence the effect of model accuracy. Consequently, quadratic polynomial models reveal a significant relationship between the recovery of Fe, Al, and Na and the independent variables (standard deviation < 5%).

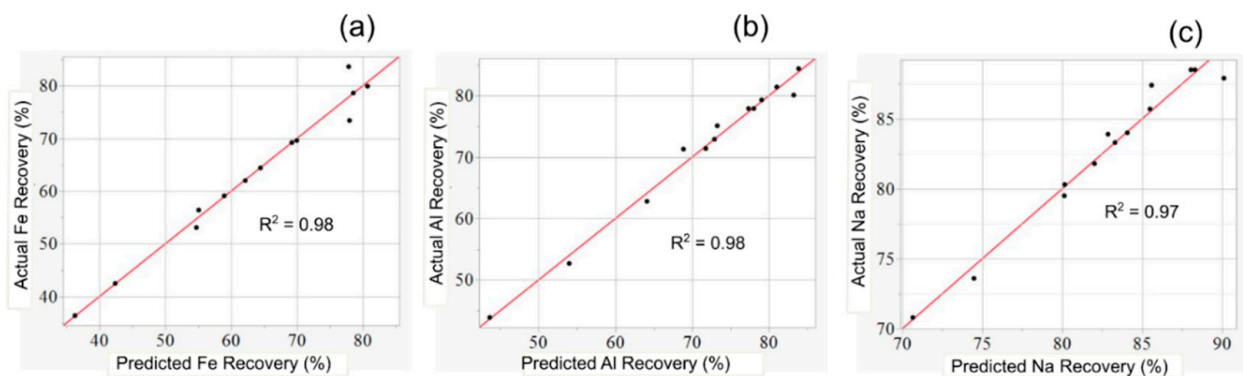
**Table 2.** Statistics summary of simulated results.

Source	Variable	$R^2$	Adj. $R^2$	SD
Quadratic	Fe recovery	0.98	0.90	4.4
	Al recovery	0.98	0.94	2.8
	Na recovery	0.97	0.88	1.9

#### 3.2. ANOVA Analysis

From the analysis of variance (ANOVA), the F-values for the quadratic models of Fe, Al, and Na recovery are 13.3, 23.6, and 11, respectively, indicating that these models are significant. There is a 2% probability that these significant "F-values" are caused by noise for Fe recovery, 1% for Al recovery, and 0.7% for Na recovery. The F-value in one-way in DoE helps us to find out if the average values of the two groups are significantly different from each other. It also gives us a  $p$ -value, which tells the probability of obtaining a result as extreme as the one we observed ( $p$ -values < 0.05 indicates significance) [11].

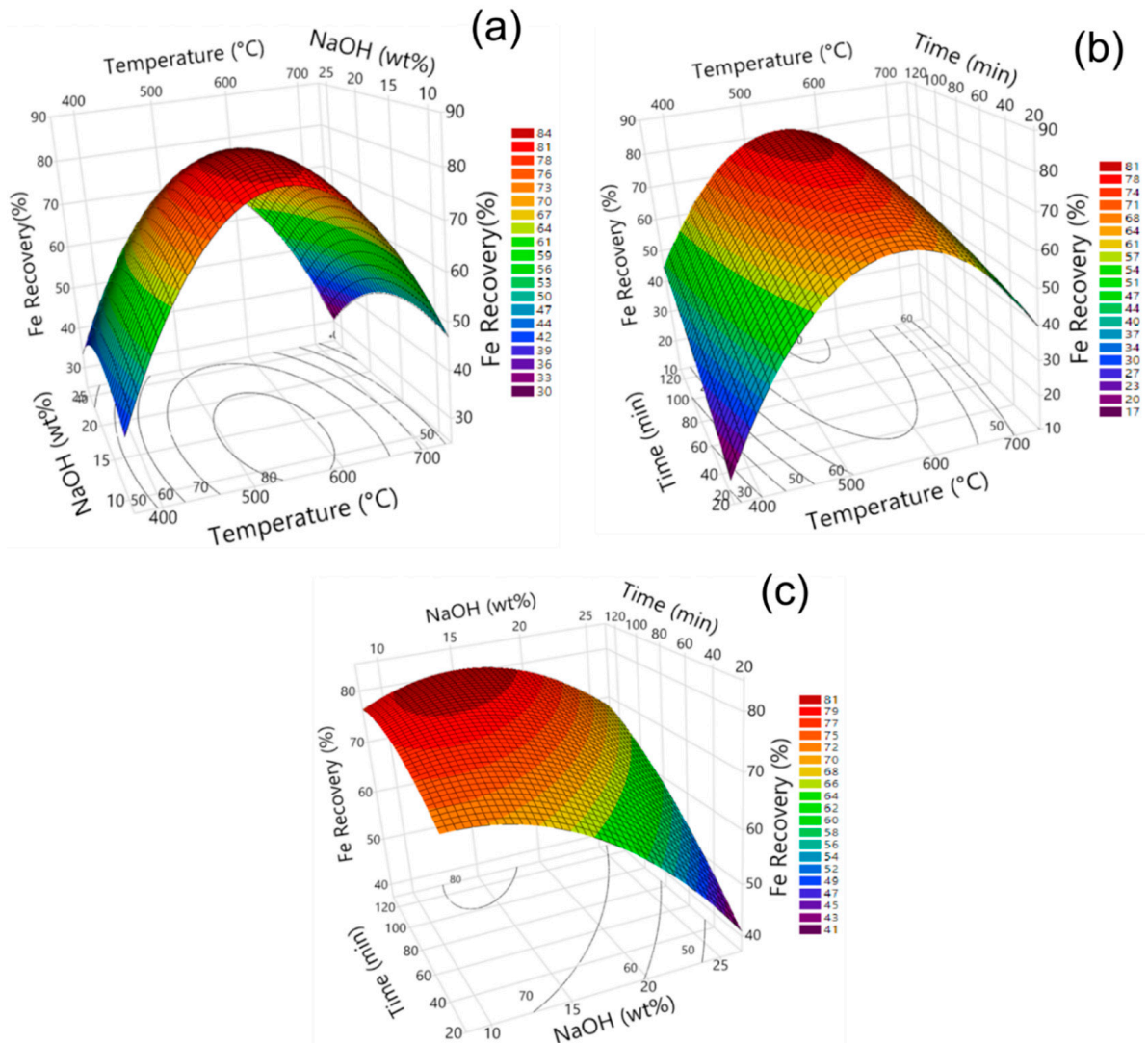
The linear terms of NaOH addition ( $x_2$ ) and time ( $x_3$ ) and the quadratic term of temperature ( $x_1$ ) are significant model terms for Fe recovery. The linear terms of temperature ( $x_1$ ) and time ( $x_3$ ) and the quadratic-term of temperature ( $x_1$ ) are significant for the Al recovery. In addition, for the Na recovery, the linear term of temperature ( $x_1$ ) and the quadratic term of temperature ( $x_1$ ) are significant input variables. The above-mentioned model terms are appropriate for estimating the Fe, Al, and Na recoveries within the confidence interval (<0.05). The correlation between observed and expected response values are depicted in Figure 2. The fact that the values predicted by the assessment models are quite close to the values actually observed implies that the regression models used to predict the responses are accurate at forecasting the responses.



**Figure 2.** The correlation between predicted and actual values of (a) Fe recovery, (b) Al recovery, and (c) Na recovery.

### 3.3. Influence of Model Parameters on Fe, Al, and Na Recovery

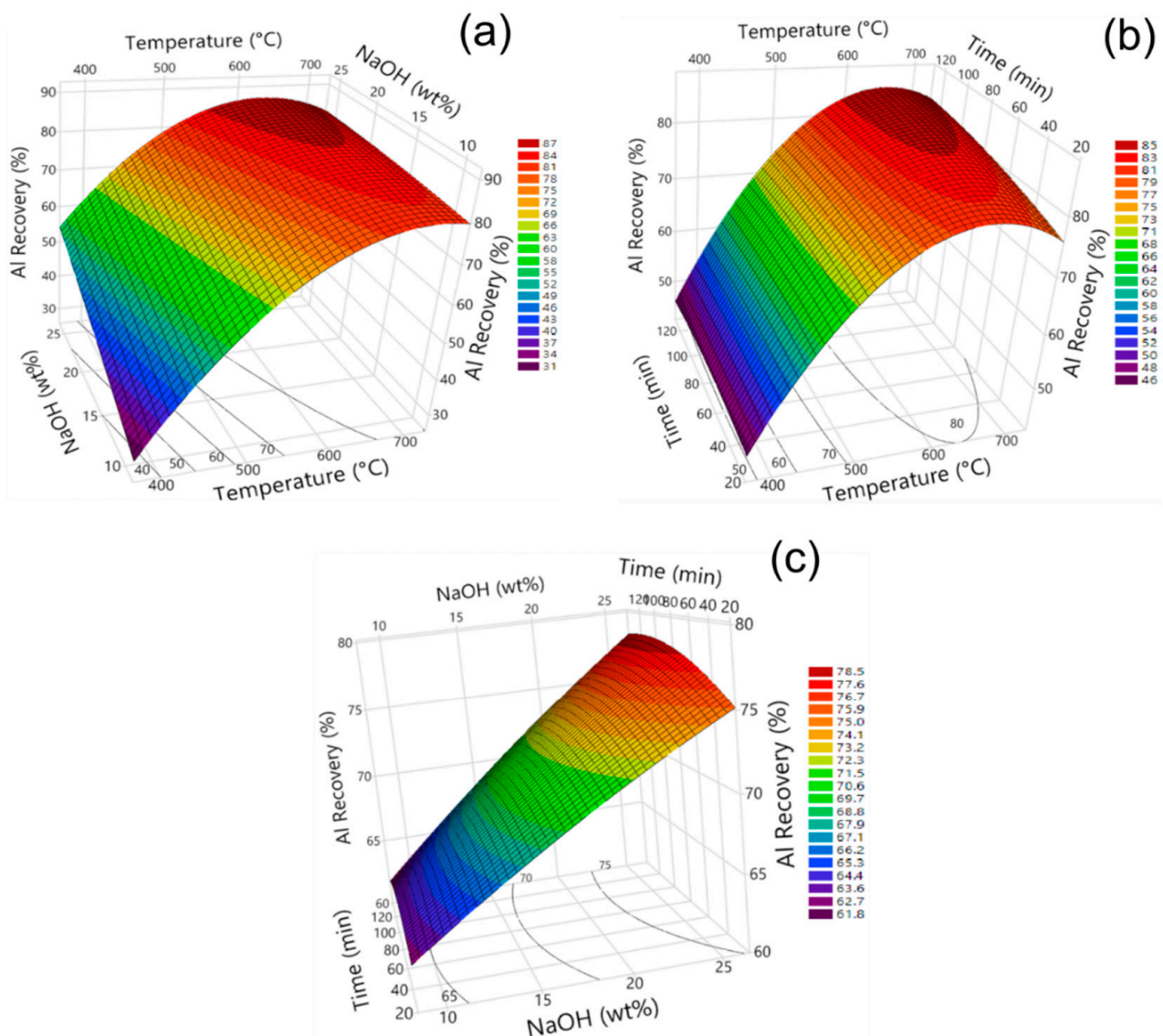
Figures 3–5 illustrate the effect of model parameters on the recovery of Fe, Al, and Na via response surface 3D plots. With a rise in temperature to 600 °C (Figure 3a), Fe recovery shows a substantial increase, followed by a decline. In addition, when the concentration of NaOH increased, 15% NaOH produced the highest recovery. Therefore, at a maximum temperature of 600 °C and a concentration of 15 wt% NaOH, Fe recovery can be maximized.



**Figure 3.** Response surface 3D plots illustrating the effects of process parameters on Fe recovery: (a) temperature–NaOH; (b) temperature–time; (c) NaOH–time.

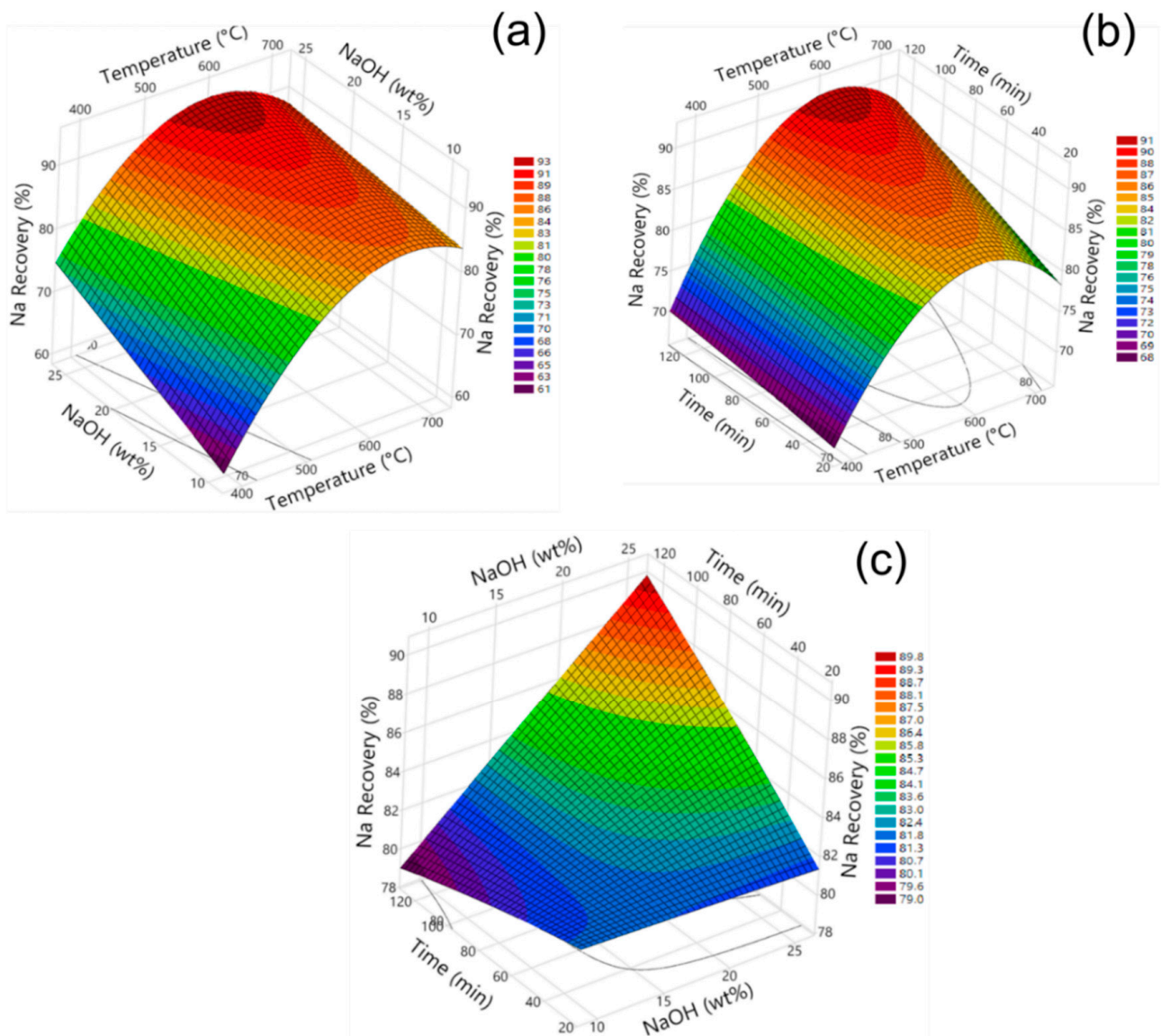
The Fe recovery exhibits an upward trend (Figure 3b) till 600 °C, while increasing with time. In addition, the maximum reduction duration and NaOH addition of 15% yield the highest Fe recovery (Figure 3c).

Figure 4 indicates the effect of model process variables on Al recovery by employing the response surface 3D plots. At the maximum reduction temperature and NaOH addition, the highest Al recovery rate was observed (Figure 4a). According to ANOVA analysis, NaOH addition and temperature variables showed a significant effect on the model. In addition, Al recovery increases with the increasing temperature and time (Figure 4b). Furthermore, the highest recovery was enhanced with a longer reduction time and NaOH addition (Figure 4c). Overall, the maximum Al recovery was concentrated at the highest temperature and NaOH addition along with the reduction time factor.



**Figure 4.** Response surface 3D plots illustrating the effects of process parameters on Al recovery: (a) temperature–NaOH; (b) temperature–time; (c) NaOH–time.

In Figure 5, the relationship between Na recovery and different input variables is depicted using three-dimensional response surface plots. The maximum Na recovery is concentrated at a temperature of 500–600 °C, while it increased with an increase in NaOH (Figure 5a). The maximum recovery was noted at 600 °C and increased with time (Figure 5c). As demonstrated in Figure 5c, the highest recovery of Na increased with increasing NaOH addition and reduction time. However, both NaOH addition and reduction time were not as significant parameters as the temperature, according to the ANOVA analysis. The highest recovery of Na was predominantly observed when the experiments involved elevated temperatures, higher NaOH additions, and extended reduction time [12].



**Figure 5.** Response surface 3D plots illustrating the effects of process parameters on Na recovery: (a) temperature–NaOH; (b) temperature–time; (c) NaOH–time.

### 3.4. Process Optimization and Validation

One objective of this research was to develop a model for optimizing the process parameters of simultaneous Fe, Al, and Na recovery. After predicting the response under optimal conditions in a full factorial design using quadratic models, confirmation experiments were conducted to validate the prediction. The optimal process parameters were a reduction temperature of 600 °C, 20 wt% of NaOH, and a reduction time of 120 min, with the predicted Fe, Al, and Na recovery of 75.8%, 84%, and 90%, respectively. However, the actual experimental observed values of Fe, Al, and Na recovery rates were 73.4%, 80.1%, and 87.9%, respectively (Table 3). The respective deviations of Fe, Al, and Na recoveries were 2.4%, 3.9%, and 2.1%, respectively. Compared to the projected outcomes, the actual values demonstrated that the optimal process parameters of multi-response acquired by JMP Pro software Version 17 were sufficiently precise and within acceptable deviation (<5%). Overall, for the simultaneous recovery of Fe, Al, and Na, parameters such as temperature and NaOH addition are more significant than reduction time.

**Table 3.** Predicted and actual Fe, Al, and Na recovery values at optimized parameters (reduction temperature: 600 °C; NaOH addition: 20 wt%; and reduction time: 120 min).

Item	Fe Recovery (%)	Range in Fe Recovery (%)	Al Recovery (%)	Range in Al Recovery (%)	Na Recovery (%)	Range in Na Recovery (%)
Predicted	75.8	67–84	84	78–89	90	96–94
Actual	73.4	--	80.1	--	87.9	--
Deviation	−2.4	--	−3.9	--	−2.1	--

#### 4. Conclusions and Remarks

This study developed an assessment model using response surface methodology to optimize the process parameters for the simultaneous recovery of Fe, Al, and Na from BR. The proposed method involves a H<sub>2</sub> reduction roasting process at low temperatures (<700 °C) and combined water leaching and wet magnetic separation. The results indicated that the recovery rates of Fe, Al, and Na were significantly influenced by temperature and NaOH addition. The optimized process parameters, determined through the model, were a reduction temperature of 600 °C, 20 wt% NaOH addition, and a reduction time of 120 min. The predicted recovery rates for Fe, Al, and Na are 75.8%, 84%, and 90%, respectively. Remarkably, the experimental observations align closely with the predicted values (<5% deviation), further validating the effectiveness of the proposed methodology.

**Author Contributions:** Conceptualization, G.P., T.H. and Y.P.; methodology, G.P., T.H. and Y.P.; software, G.P.; validation, T.H. and Y.P.; formal analysis, G.P.; investigation, G.P.; resources, Y.P.; data curation, G.P., T.H. and Y.P.; writing—original draft preparation, G.P.; writing—review and editing, T.H. and Y.P.; visualization, G.P.; supervision, T.H. and Y.P.; project administration, Y.P. All authors have read and agreed to the published version of the manuscript.

**Funding:** This project has received funding from the European Union’s Horizon 2020 research and innovation programme under grant agreement No. 958307. The project website is <https://h2020harare.eu/> (accessed on 1 July 2023).

**Institutional Review Board Statement:** Not applicable.

**Informed Consent Statement:** Not applicable.

**Data Availability Statement:** Dataset available on request from the authors.

**Conflicts of Interest:** The authors declare no conflicts of interest.

#### References

- Evans, K. The History, Challenges, and New Developments in the Management and Use of Bauxite Residue. *J. Sustain. Met.* **2016**, *2*, 316–331. [[CrossRef](#)]
- Liu, X.; Han, Y.; He, F.; Gao, P.; Yuan, S. Characteristic, hazard, and iron recovery technology of red mud—A critical review. *J. Hazard. Mater.* **2021**, *420*, 126542. [[CrossRef](#)]
- Hassanzadeh, A.; Pilla, G.; Kar, M.K.; Kowalczyk, P.B. An Invitation on Characterization of H<sub>2</sub>-Reduced Bauxite Residue and Recovering Iron through Wet Magnetic Separation Processes. *Minerals* **2023**, *13*, 728. [[CrossRef](#)]
- Kapelari, S.; Gamaletsos, P.N.; Pilla, G.; Pontikes, Y.; Blanpain, B. Developing a Low-Temperature, Carbon-Lean Hybrid Valorisation Process for Bauxite Residue (Red Mud) Towards Metallic Fe and Al Recovery. *J. Sustain. Metall.* **2023**, *9*, 578–587. [[CrossRef](#)]
- Borra, C.R.; Blanpain, B.; Pontikes, Y.; Binnemans, K.; Van Gerven, T. Recovery of Rare Earths and Major Metals from Bauxite Residue (Red Mud) by Alkali Roasting, Smelting, and Leaching. *J. Sustain. Met.* **2016**, *3*, 393–404. [[CrossRef](#)]
- Cardenia, C.; Balomenos, E.; Pnias, D. Iron Recovery from Bauxite Residue through Reductive Roasting and Wet Magnetic Separation. *J. Sustain. Met.* **2018**, *5*, 9–19. [[CrossRef](#)]
- Samouhos, M.; Taxiarchou, M.; Pilatos, G.; Tsakiridis, P.; Devlin, E.; Pissas, M. Controlled reduction of red mud by H<sub>2</sub> followed by magnetic separation. *Miner. Eng.* **2017**, *105*, 36–43. [[CrossRef](#)]
- Pilla, G.; Kapelari, S.V.; Hertel, T.; Blanpain, B.; Pontikes, Y. Hydrogen reduction of bauxite residue and selective metal recovery. *Mater. Today Proc.* **2022**, *57*, 705–710. [[CrossRef](#)]

9. Pilla, G.; Hertel, T.; Kapelari, S.; Blanpain, B.; Pontikes, Y. Reactions and phase transformations during the low-temperature reduction of bauxite residue by H<sub>2</sub> in the presence of NaOH, and recovery rates downstream. In Proceedings of the 40th International ICSOBA Conference, Athens, Greece, 10–14 October 2022.
10. Anawati, J.; Azimi, G. Integrated carbothermic smelting–Acid baking–Water leaching process for extraction of scandium, aluminum, and iron from bauxite residue. *J. Clean. Prod.* **2022**, *330*, 129905. [[CrossRef](#)]
11. Wang, R.; Liu, Z.; Chu, M.; Wang, H.-T.; Zhao, W.; Gao, L.-H. Modeling assessment of recovering iron from red mud by direct reduction: Magnetic separation based on response surface methodology. *J. Iron Steel Res. Int.* **2018**, *25*, 497–505. [[CrossRef](#)]
12. Hassanzadeh, A.; Pilla, G.; Hertel, T.; Pontikes, Y.; Kowalczyk, P.B. H<sub>2</sub>-reduction of bauxite residue and iron recovery through magnetic separation. In Proceedings of the 17th International Mineral Processing Symposium, İstanbul, Turkey, 15 December 2022; Turkish Mining Development Foundation: İstanbul, Turkey; pp. 233–243.

**Disclaimer/Publisher’s Note:** The statements, opinions and data contained in all publications are solely those of the individual author(s) and contributor(s) and not of MDPI and/or the editor(s). MDPI and/or the editor(s) disclaim responsibility for any injury to people or property resulting from any ideas, methods, instructions or products referred to in the content.